

# A Worldsheet Description of Planar Yang-Mills Theory\*

Charles B. Thorn<sup>†</sup>

*School of Natural Science, Institute for Advanced Study, Princeton NJ 08540*

and

*Institute for Fundamental Theory*

*Department of Physics, University of Florida, Gainesville FL 32611*

## Abstract

We extend previous work by developing a worldsheet description of non-abelian gauge theory (Yang-Mills). This task requires the introduction of Grassmann variables on the world sheet analogous to those of the Neveu-Schwarz-Ramond formulation of string theory. A highlight of our construction is that once the three gluon vertices of Yang-Mills Feynman diagrams are given a worldsheet description, the worldsheet formalism automatically produces all of the quartic vertices.

---

\* This work was supported in part by the Monell Foundation and in part by the Department of Energy under Grant No. DE-FG02-97ER-41029.

<sup>†</sup>E-mail address: [thorn@phys.ufl.edu](mailto:thorn@phys.ufl.edu)

# 1 Introduction

Several months ago, Bardakci and I proposed [1] a way of expressing the planar Feynman diagrams, selected by 't Hooft's  $N_c \rightarrow \infty$  limit [2], of a quantum matrix field theory in the language of light-cone interacting string diagrams [3, 4]. As a paradigm for our method we treated the simplest example of  $\text{Tr}\phi^3$  theory, but stressed that our methods should be applicable to a wide range of quantum field theories.

In this article we extend the program to include non-abelian gauge theories (Yang-Mills theories). The extension involves several new features. The light-cone gauge ( $A_- = 0$ ) Feynman rules for gauge theories involve both cubic and quartic vertices. The cubic vertices are linear in the transverse momenta entering the vertex, and also depend on the spin of the gauge bosons. In addition, the contribution to the cubic vertex that arises from the elimination of the longitudinal potential  $A_+$  is a rational function of the  $p_i^+$  entering the vertex. The quartic vertices don't depend on the transverse momentum, but they are spin dependent and the induced "Coulomb exchange" quartic is a rational function of the  $p_i^+$  entering the vertex. Thus the worldsheet description must describe, in addition to the flow of momentum through a complicated planar graph, the flow of gluon spin through the graph. Further, the cubic vertices display a spin-orbit coupling.

We shall introduce vector-valued Grassmann variables  $\mathbf{S}_{1,2}(\sigma, \tau)$  of the Neveu-Schwarz-Ramond type to keep track of the spin flow in a large diagram. In addition to contributing to the bulk worldsheet action, these variables appear in insertion factors at the interaction points of the worldsheet. These insertion factors provide the necessary momentum and spin dependence of the cubic vertices. We shall also need to supplement the ghost system introduced in [1] to locally describe the new factors of  $p^+$  that occur in the vertices. We use an  $x^+, p^+$  lattice to give a concrete meaning to our construction, especially at interaction points on the world sheet. But in the bulk of the world sheet, away from boundaries, the worldsheet action has a rather simple formal continuum limit

$$S = \int d\tau d\sigma \left[ \frac{\mathbf{q}'^2}{2} + \bar{\mathbf{S}}_2 \cdot \mathbf{S}'_2 - \bar{\mathbf{S}}_1 \cdot \mathbf{S}'_1 + \text{Ghost Terms} \right]. \quad (1)$$

Here the prime denotes  $\partial/\partial\sigma$ . The bosonic worldsheet variable  $\mathbf{q}$  was introduced in [1]. Its derivative is the density of transverse momentum on a bit of world sheet: that is  $\mathbf{q}'d\sigma$  is the transverse momentum carried by the element  $d\sigma$ . The noteworthy feature here is that there are no time derivatives in the bulk: all dynamics occurs at the boundaries of the worldsheet.

For the quartic vertices of the usual Feynman rules, the worldsheet formalism provides a pleasant surprise. Initially it seemed evident that a quartic vertex would introduce nonlocal elements into the worldsheet description. This is because four worldsheet strips of varying width, corresponding to the different  $p_i^+$  carried by each external leg into a vertex, can't be glued together at a point. It is therefore gratifying that these quartic vertices are produced from pairs of cubic vertices by the worldsheet formalism. This comes about as follows. The worldsheet description of the cubic vertex, which is linear in the transverse momentum, requires the insertion of a factor of  $\mathbf{q}'(\sigma_1, \tau_1)$  for  $\sigma_1, \tau_1$  near the interaction point. When a four point amplitude is built from cubics there are two such insertions at  $\sigma_1, \tau_1$  and  $\sigma_2, \tau_2$ , say. When  $\tau_1 \neq \tau_2$  this double insertion just provides the momentum factors for the two cubic vertices. However, for  $\tau_1 = \tau_2$  the double insertion provides an additional "quantum fluctuation" term whose value precisely gives the quartic vertex. Since the quartic vertices are taken care of by the locally specified worldsheet formalism, no worldsheet nonlocal elements need be introduced.

In Section 2 we review the worldsheet construction for the scalar theory given in Ref. [1], making some minor adjustments that will be helpful for the Yang-Mills construction. Section 3 contains

the main result of the paper, the extension of the worldsheet formalism to Yang-Mills theories. Section 4 contains concluding remarks.

## 2 Review of Scalar Theory<sup>†</sup>

### 2.1 Propagator

We use light-cone coordinates defined as  $x^\pm = (x^0 \pm x^3)/\sqrt{2}$ . The remaining components of  $x^\mu$  will be distinguished by Latin indices, or as a vector by bold-face type. The components of any four vector  $v^\mu$  will be  $(v^+, v^-, \mathbf{v})$  or  $(v^+, v^-, v^k)$ . The Lorentz invariant scalar product of two four vectors  $v, w$  is written  $v \cdot w = \mathbf{v} \cdot \mathbf{w} - v^+ w^- - v^- w^+$ . We shall select  $x^+$  to be our quantum evolution parameter, and we recall that the Hamiltonian conjugate to this time is  $p^-$ . A massless on-shell particle thus has the “energy”  $p^- = \mathbf{p}^2/2p^+$ .

Central to the worldsheet construction of [1] is the mixed representation  $(x^+, p^+, \mathbf{p})$  of the propagator of the free massless scalar field [2]:

$$\Delta(\mathbf{p}, p^+, x^+) \equiv \int \frac{dp^-}{2\pi i} e^{-ix^+ p^-} \frac{1}{p^2 - i\epsilon} = \frac{\theta(x^+)}{2p^+} e^{-ix^+ \mathbf{p}^2/2p^+} \rightarrow \frac{\theta(\tau)}{2p^+} e^{-\tau \mathbf{p}^2/2p^+}, \quad (2)$$

where we assume  $p^+ > 0$ . Since we consider only planar diagrams in this paper, we may suppress explicit reference to color indices. Note that we have defined imaginary time  $\tau = ix^+$ . We use imaginary  $x^+$  for convenience to make integrals damped instead of rapidly oscillating.

We set up a lattice worldsheet [4] by discretizing  $\tau$  and  $p^+$ :

$$\tau = ka, \quad p^+ = lm, \quad \text{for } k, l = 1, 2, 3, \dots \quad (3)$$

Then the scalar propagator becomes

$$\Delta \rightarrow \frac{\theta(k)}{2lm} e^{-k(a/m)\mathbf{p}^2/2l} \quad (4)$$

According to the traditional Feynman rules each propagator momentum is integrated with measure  $dp^+ d\mathbf{p}/(2\pi)^3$ . Combining the  $1/2p^+$  factor with this measure produces

$$\int \frac{dp^+}{2p^+} \int \frac{d\mathbf{p}}{(2\pi)^3} \rightarrow \sum_l \int \frac{d\mathbf{p}}{2l(2\pi)^3}. \quad (5)$$

In our construction we associate the factor  $1/2l(2\pi)^3$  with one or both of the two vertices to which the line is attached. We shall distribute the purely numerical factors symmetrically between the two vertices, an  $n$ -leg vertex receiving a factor  $1/(16\pi^3)^{n/2}$ . Each vertex is also integrated with measure

$$\int d\tau (2\pi)^3 \delta\left(\sum p_i^+\right) \delta\left(\sum \mathbf{p}_i\right) \rightarrow \sum_k \frac{(2\pi)^3 a}{m} \delta_{l_1+l_2+l_3, 0} \delta\left(\sum \mathbf{p}_i\right).$$

We shall suppress the delta functions but include the numerical factors in the vertex. Thus all together each  $n$ -leg vertex is multiplied by the numerical factors  $a/2m(16\pi^3)^{(n-2)/2}$ . For cubics this factor is just  $a/8m\pi^{3/2}$  and for quartics it is  $a/32m\pi^3$ .

In contrast, we assign the factor  $1/l$  asymmetrically to only one of the two vertices attached to the propagator. Since in light-cone quantization all propagation is forward in time, we can

---

<sup>†</sup>The new features in this review of Ref. [1] were developed in collaboration with K. Bardakci.

consistently assign the factor to the *earlier* of the two vertices connected by the line. Then a *fission* vertex, in which one particle with  $p^+ = lm$  “decays” to two particles with  $p_1^+ = l_1m$ ,  $p_2^+ = l_2m$  will be assigned the factor  $1/l_1l_2$ , whereas a *fusion* vertex, which is the time-reversal of the fission vertex, will be assigned the factor  $1/l$ . All propagators are then simple exponentials  $e^{-kap^2/2lm}$ .

Consider a line carrying  $M$  units of  $p^+$ . As in [2] we write the total momentum as a difference  $\mathbf{p} \equiv \mathbf{q}_M - \mathbf{q}_0$ . We also must introduce ghost variables  $b, c$  on each lattice site to provide crucial factors of  $M$  when we represent a single gluon as  $M$  bits. We make use of the ghost integrals

$$\int \prod_{i=1}^{M-1} \frac{dc_i db_i}{2\pi} \exp \left\{ \frac{a}{m} \left[ b_1 c_1 + b_{M-1} c_{M-1} + \sum_{i=1}^{M-2} (b_{i+1} - b_i)(c_{i+1} - c_i) \right] \right\} = M \left( \frac{a}{2\pi m} \right)^{M-1} \quad (6)$$

For simplicity of presentation, we restrict attention to the case  $d = 2$ , four dimensional space-time. Then we only require one  $b, c$  set of ghosts. Thus for each time slice introduce the action

$$S = S_g + S_q \quad (7)$$

$$S_q = \frac{a}{2m} \sum_j \sum_{i=0}^{M-1} (\mathbf{q}_{i+1}^j - \mathbf{q}_i^j)^2 \quad (8)$$

$$S_g = -\frac{a}{m} \sum_j \left[ b_1^j c_1^j + b_{M-1}^j c_{M-1}^j + \sum_{i=1}^{M-2} (b_{i+1}^j - b_i^j)(c_{i+1}^j - c_i^j) \right] \quad (9)$$

Then

$$\exp \left\{ -N \frac{a}{m} \frac{(\mathbf{q}_M - \mathbf{q}_0)^2}{2M} \right\} = \int \prod_{j=1}^N \prod_{i=1}^{M-1} \frac{dc_i^j db_i^j}{2\pi} d\mathbf{q}_i^j e^{-S_g - S_q} \equiv \int DcDbD\mathbf{q} e^{-S}. \quad (10)$$

In (10) we have imposed Dirichlet boundary conditions  $\mathbf{q}_{0,j} = \mathbf{q}_0$  and  $\mathbf{q}_{M,j} = \mathbf{q}_M$ . However, to dynamically implement momentum conservation in the path integral we integrate over  $q_M^j$  independently, retain the Dirichlet boundary condition at  $i = 0$ , where we impose  $\mathbf{q}_0^j = \mathbf{q}_0$ , but insert momentum conserving delta functions at the other end  $i = M$ . It is convenient but not necessary to set  $\mathbf{q}_0 = 0$ . For formal uniformity we also introduce extra ghost variables  $b_M^j, c_M^j$  which we integrate over with weight  $\exp 2\pi \sum_j b_M^j c_M^j$ , which just amounts to inserting a factor of unity in the path integral. The path integral for the free propagator is then given for  $d = 2$  by

$$T_{fi} = \int \prod_{j=1}^N \prod_{i=1}^M \frac{dc_i^j db_i^j}{2\pi} d\mathbf{q}_i^j \prod_{j=0}^N \frac{d\mathbf{y}_M^j}{(2\pi)^2} \exp \left\{ -S + 2\pi \sum_j b_M^j c_M^j - i \sum_{j=0}^N \mathbf{y}_M^j \cdot (\mathbf{q}_M^{j+1} - \mathbf{q}_M^j) \right\} \quad (11)$$

When we draw discretized worldsheet diagrams (see Fig. 1), with time flowing up, we shall distinguish the bulk and boundary degrees of freedom by dotted and solid vertical lines respectively.

## 2.2 Cubic Interactions

In this subsection we review the world sheet construction of the cubic vertices in the planar diagrams of  $g\text{Tr}\phi^3/3\sqrt{N_c}$  theory. A fission vertex describes a field quantum with momenta  $\mathbf{Q}, Mm$  transforming to two field quanta with momenta  $\mathbf{p}, lm; (\mathbf{Q} - \mathbf{p}), (M-l)m$ . Before the interaction we have a single propagator treated as in Section 2.1. After the interaction we have two propagators. We assign the factor  $ga/8l(M-l)m\pi^{3/2}$  to the vertex. The factors  $1/l(M-l)$  must be incorporated by a worldsheet local treatment of the fission point.

This is done by altering the ghost integral near the interaction point to force the ghost integral to give unity instead of a factor of  $M$  or  $l(M-l)$ . For example, deleting the  $i = M-1$  (or  $i = 0$ ) term in the exponential of (6) has precisely this effect:

$$\int \prod_{i=1}^{M-1} \frac{dc_i db_i}{2\pi} \exp \left\{ \frac{a}{m} \left[ b_1 c_1 + \sum_{i=1}^{M-2} (b_{i+1} - b_i)(c_{i+1} - c_i) \right] \right\} = \left( \frac{a}{2\pi m} \right)^{M-1} \quad (12)$$

$$\int \prod_{i=1}^{M-1} \frac{dc_i db_i}{2\pi} \exp \left\{ \frac{a}{m} \left[ b_{M-1} c_{M-1} + \sum_{i=1}^{M-2} (b_{i+1} - b_i)(c_{i+1} - c_i) \right] \right\} = \left( \frac{a}{2\pi m} \right)^{M-1} \quad (13)$$

Note, by the way, that if both the first and last terms are deleted the result is zero:

$$\int \prod_{i=1}^{M-1} \frac{dc_i db_i}{2\pi} \exp \left\{ \frac{a}{m} \sum_{i=1}^{M-2} (b_{i+1} - b_i)(c_{i+1} - c_i) \right\} = 0. \quad (14)$$

This fact will be important in the worldsheet construction for Yang-Mills theory. We also get unity if we delete some interior ghost coupling term labeled by  $k$

$$\int \prod_{i=1}^{M-1} \frac{dc_i db_i}{2\pi} \exp \left\{ \frac{a}{m} \left[ b_1 c_1 + b_{M-1} c_{M-1} + \sum_{\substack{i=1 \\ i \neq k}}^{M-2} (b_{i+1} - b_i)(c_{i+1} - c_i) \right] \right\} = \left( \frac{a}{2\pi m} \right)^{M-1}. \quad (15)$$

So for the fission vertex, we choose to delete the corresponding terms on both sides of the interaction point on the time slice just after the fission, and this will lead to a factor  $1/l(M-l)$ . By the same token if we delete a coupling term just after a fusion vertex and, say, just to the right of the interaction point, we obtain the factor  $1/M$ . The fission vertex is represented by a time line on which the momentum is constant. That is, the momentum on this line is fixed (Dirichlet condition), but in a loop this fixed value is integrated. Similarly, the ghost fields on this line are fixed at zero. As a concrete example, we give all the necessary factors for the vertices, the ends of solid lines, in the context of the one loop correction to the propagator, shown in Fig. 1.

Since we require independent ghost variables at the circled sites, we insist on the restriction  $l \geq 2$ . Applying the above considerations to this diagram, we have, omitting for compactness the delta functions that implement the Dirichlet conditions on the boundary  $i = M$ ,

$$\begin{aligned} T_{fi}^{\text{one loop II}} &= \int \prod_{j=1}^N \prod_{i=1}^{M-1} \frac{dc_i^j db_i^j}{2\pi} d^2 q_i^j e^{-S} \frac{g^2}{16\pi} \prod_{j=k+2}^{k+l} \delta(\mathbf{q}_{M_1}^j - \mathbf{q}_{M_1}^{j-1}) \prod_{j=k+2}^{k+l-1} \left[ 2\pi \delta(b_{M_1}^j) \delta(c_{M_1}^j) \right] \\ &\exp \left\{ -\frac{a}{m} \sum_{j=k+1}^{k+l} \left[ 2b_{M_1}^j c_{M_1}^j - (b_{M_1-1}^j + b_{M_1+1}^j) c_{M_1}^j - b_{M_1}^j (c_{M_1-1}^j + c_{M_1+1}^j) \right] \right\} \\ &\exp \left\{ \frac{a}{m} \left[ b_{M_1}^{k+1} c_{M_1}^{k+1} - b_{M_1-1}^{k+1} c_{M_1-1}^{k+1} - b_{M_1+1}^{k+1} c_{M_1+1}^{k+1} \right] \right\} \\ &\exp \left\{ \frac{a}{m} \left[ b_{M_1}^{k+l} c_{M_1}^{k+l} - (b_{M_1+1}^{k+l+1} - b_{M_1}^{k+l+1}) (c_{M_1+1}^{k+l+1} - c_{M_1}^{k+l+1}) \right] \right\} \quad (16) \end{aligned}$$

The superscript  $II$  signifies that we have made minor changes compared to Ref. [1]. In this new alternative, we associate factors

$$\mathcal{V}_0 \equiv \frac{ga}{4m\sqrt{\pi}} \exp \left\{ -\frac{a}{m} (b_{M_1-1}^{k+1} c_{M_1-1}^{k+1} + b_{M_1+1}^{k+1} c_{M_1+1}^{k+1}) \right\} \quad (17)$$

$$\bar{\mathcal{V}}_0 \equiv \frac{ga}{4m\sqrt{\pi}} \exp \left\{ -\frac{a}{m} (b_{M_1+1}^{k+l+1} - b_{M_1}^{k+l+1}) (c_{M_1+1}^{k+l+1} - c_{M_1}^{k+l+1}) \right\} \quad (18)$$

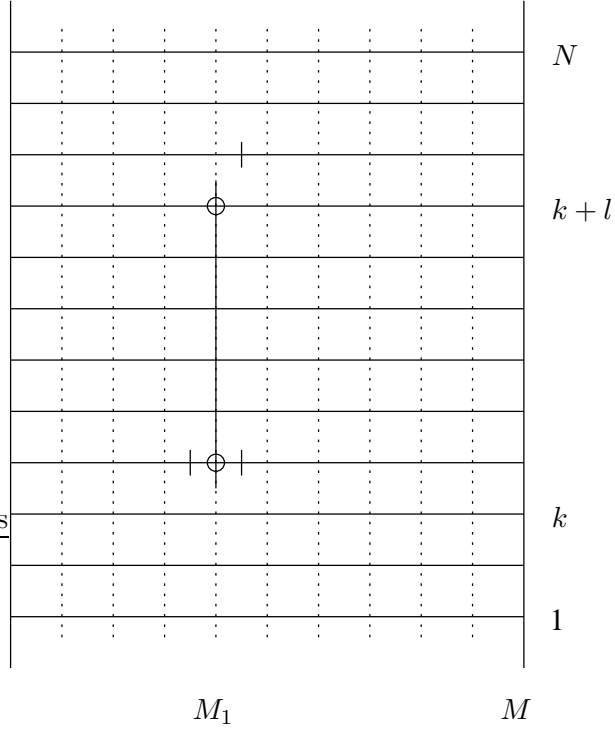


Figure 1: One loop correction to the propagator. The momenta on the sites crossed by the solid vertical line are all equal. The tick marks on the horizontal links just after the interaction points indicate the deleted ghost terms. The ghost terms associated with the circled sites are coupled to the vertex insertions.

with the fission and fusion vertices respectively, the different forms due to the asymmetric way we have assigned  $1/p^+$  factors to the vertices. Note that since the factor on the second line of Eq. 16 explicitly removes all the dependence on  $b_{M_1}^j, c_{M_1}^j$  for  $k+1 \leq j \leq k+l$  from  $S$ , we are free to substitute

$$\prod_{j=k+2}^{k+l-1} \left[ 2\pi \delta(b_{M_1}^j) \delta(c_{M_1}^j) \right] \rightarrow \exp \left\{ 2\pi \sum_{j=k+2}^{k+l-1} b_{M_1}^j c_{M_1}^j \right\}, \quad (19)$$

which treats the interior solid line similarly to the way we treated the boundary at  $i = M$ . Then one can write the compact expression

$$T_{fi}^{\text{one loop II}} = \int \prod_{j=1}^N \prod_{i=1}^{M-1} \frac{dc_i^j db_i^j}{2\pi} d^2 q_i^j \prod_{j=k+2}^{k+l} \delta(\mathbf{q}_{M_1}^j - \mathbf{q}_{M_1}^{j-1}) \exp \left\{ -S + b_{M_1}^{k+1} c_{M_1}^{k+1} \mathcal{V}_0 + b_{M_1}^{k+l} c_{M_1}^{k+l} \bar{\mathcal{V}}_0 \right\} \\ \exp \left\{ 2\pi \sum_{j=k+2}^{k+l-1} b_{M_1}^j c_{M_1}^j - \frac{a}{m} \sum_{j=k+1}^{k+l} \left[ 2b_{M_1}^j c_{M_1}^j - (b_{M_1-1}^j + b_{M_1+1}^j) c_{M_1}^j - b_{M_1}^j (c_{M_1-1}^j + c_{M_1+1}^j) \right] \right\} \quad (20)$$

The next step is to write a formula that systematically sums over all the planar diagrams on the lattice. The general planar diagram has an arbitrary number of vertical solid lines. An interior

link  $j$  of a solid line at  $i = M_1$  is represented by the product of delta functions

$$\delta(\mathbf{q}_i^j - \mathbf{q}_i^{j-1}) = \int \frac{d\mathbf{y}_i^j}{(2\pi)^2} e^{i\mathbf{y}_i^j \cdot (\mathbf{q}_i^j - \mathbf{q}_i^{j-1})}, \quad (21)$$

and by the  $j$ th term in the exponent of the last line of Eq. 20. A simple way to supply such factors is to assign an Ising spin  $s_i^j = \pm 1$  to each site of the lattice. We assign  $+1$  if the site  $(i, j)$  is crossed by a vertical solid line,  $-1$  otherwise. Then we can represent both kinds of link, solid line and dotted line by the unified factor

$$\int \frac{d\mathbf{y}_i^j}{(2\pi)^2} \exp \left\{ i\mathbf{y}_i^j \cdot (\mathbf{q}_i^j - \mathbf{q}_i^{j-1}) P_i^j P_i^{j-1} + \ln(4\pi^2/V)(1 - P_i^j P_i^{j-1}) \right\} \\ \times \exp \left\{ 2\pi P_i^{j-1} P_i^j P_i^{j+1} b_i^j c_i^j - \frac{a}{m} P_i^j \left[ 2b_i^j c_i^j - (b_{i-1}^j + b_{i+1}^j) c_i^j - b_i^j (c_{i-1}^j + c_{i+1}^j) \right] \right\}, \quad (22)$$

where we have defined the projector  $P_i^j = (1 + s_i^j)/2$  and where  $V$  is the volume of transverse space. Note that the way we have multiplied different terms by different projection operators ensures that the ranges of summation are precisely as in our one-loop formula.

At the endpoints of each solid line we have to supply the vertex insertions  $\mathcal{V}_0, \bar{\mathcal{V}}_0$ . These factors occur when  $s_i^j = -s_i^{j-1}$ . So in the exponent we multiply the factors by  $P_i^j P_i^{j+1} (1 - P_i^{j-1})$ ,  $P_i^j P_i^{j-1} (1 - P_i^{j+1})$  respectively. Again, the extra projection operators are such as to suppress solid lines which cross only one horizontal line. That is, they enforce the requirement that each internal loop occupies at least two time steps:  $l \geq 2$ .

Our final formula for the sum of all planar diagrams is therefore

$$T_{fi}^{II} = \sum_{s_i^j = \pm 1} \int DcDbDyD\mathbf{q} \exp \left\{ -S + \sum_{i,j} b_i^j c_i^j P_i^j \left[ \mathcal{V}_{0i}^j P_i^{j+1} (1 - P_i^{j-1}) + \bar{\mathcal{V}}_{0i}^j P_i^{j-1} (1 - P_i^{j+1}) \right] \right\} \\ \exp \left\{ \sum_{i,j} \left[ i\mathbf{y}_i^j \cdot (\mathbf{q}_i^j - \mathbf{q}_i^{j-1}) P_i^j P_i^{j-1} + \ln(4\pi^2/V)(1 - P_i^j P_i^{j-1}) \right] \right\} \\ \exp \left\{ \sum_{i,j} P_i^j \left[ 2\pi P_i^{j-1} P_i^j P_i^{j+1} b_i^j c_i^j - \frac{a}{m} \left[ 2b_i^j c_i^j - (b_{i-1}^j + b_{i+1}^j) c_i^j - b_i^j (c_{i-1}^j + c_{i+1}^j) \right] \right] \right\}, \quad (23)$$

where we have defined the measure as

$$DcDbDyD\mathbf{q} \equiv \prod_{j=1}^N \prod_{i=1}^{M-1} \frac{dc_i^j db_i^j d\mathbf{y}_i^j d\mathbf{q}_i^j}{2\pi (2\pi)^2}. \quad (24)$$

The first exponent in this formula is just the action  $S$  for the free propagator plus the spin flipping terms that take into account the creation and destruction of solid lines. The second exponent takes care of the delta function insertions required for each solid line. The final exponent adjusts the ghost couplings surrounding each solid line. Notice that when  $g = 0$ , this exponential forces  $T_{fi}$  to vanish unless  $s_i^j = s_i^{j-1}$  for all  $i, j$ , because there would then not be enough ghost factors to saturate the ghost integrals. Thus solid lines are eternal if  $g = 0$ , corresponding to the free field case.

We remark that the expression (23) sums all the planar multi-loop corrections to the propagator of the matrix scalar field. The evolving system is therefore in the adjoint representation of the color

group. That is, we have tacitly assumed that the only solid lines initially and finally are those at the boundaries of the strip. More general initial and final states are described by allowing more solid lines initially and finally. When the system is in a color singlet state, we must of course include diagrams in which the outer boundaries are identified, *i.e.* the diagrams should be drawn on a cylinder, not a strip. In this case,  $\mathbf{q}(p^+) = \mathbf{q}(0) + \mathbf{p}$ , the variable  $\mathbf{q}(\sigma)$  is strictly periodic only in the state of zero total transverse momentum.

Finally, we mention an approximate treatment of the momentum delta functions on the solid lines that may be more suited to practical calculations. The idea is to use a Gaussian approximation for the delta function:

$$\delta(\mathbf{q}) = \lim_{\epsilon \rightarrow 0} \frac{1}{(2\pi\epsilon)^{d/2}} \exp \left\{ -\frac{\mathbf{q}^2}{2\epsilon} \right\}. \quad (25)$$

We can keep  $\epsilon$  finite until the end of the calculation. However, if we want to recover the exact result of using delta functions, we should send  $\epsilon \rightarrow 0$  *before* the continuum limit  $a, m \rightarrow 0$ . Using this device, our formula for the sum of planar diagrams becomes (for  $d = 2$ ):

$$\begin{aligned} T_{fi}^{II} &= \lim_{\epsilon \rightarrow 0} \sum_{s_i^j = \pm 1} \int DcDbD\mathbf{q} \exp \left\{ -S + \sum_{i,j} b_i^j c_i^j P_i^j \left[ \mathcal{V}_{0i}^j P_i^{j+1} (1 - P_i^{j-1}) + \bar{\mathcal{V}}_{0i}^j P_i^{j-1} (1 - P_i^{j+1}) \right] \right\} \\ &\exp \left\{ -\sum_{i,j} \left[ \frac{(\mathbf{q}_i^j - \mathbf{q}_i^{j-1})^2}{2\epsilon} + \ln(2\pi\epsilon) \right] P_i^j P_i^{j-1} \right\} \\ &\exp \left\{ \sum_{i,j} P_i^j \left[ 2\pi P_i^{j-1} P_i^{j+1} b_i^j c_i^j - \frac{a}{m} \left( 2b_i^j c_i^j - (b_{i-1}^j + b_{i+1}^j) c_i^j - b_i^j (c_{i-1}^j + c_{i+1}^j) \right) \right] \right\}, \end{aligned} \quad (26)$$

with the measure now given by

$$DcDbD\mathbf{q} \equiv \prod_{j=1}^N \prod_{i=1}^{M-1} \frac{dc_i^j db_i^j}{2\pi} d\mathbf{q}_i^j. \quad (27)$$

### 3 Yang-Mills

#### 3.1 Treatment of Factors of Transverse Momentum

Here, we use the notation and conventions in Ref. [5], according to which the values of the non-vanishing three transverse gluon vertices are:

$$\begin{array}{c} \begin{array}{c} \uparrow \\ \swarrow \quad \searrow \\ 1 \quad 2 \end{array} \end{array} = \frac{ga}{4m\pi^{3/2}} M_3 \left( \frac{p_2^\wedge}{M_2} - \frac{p_1^\wedge}{M_1} \right) \quad (28)$$

$$\begin{array}{c} \begin{array}{c} \downarrow \\ \swarrow \quad \searrow \\ 1 \quad 2 \end{array} \end{array} = \frac{ga}{4m\pi^{3/2}} M_3 \left( \frac{p_2^\vee}{M_2} - \frac{p_1^\vee}{M_1} \right) \quad (29)$$

Here,  $p^\wedge = (p^x + ip^y)/\sqrt{2}$ ,  $p^\vee = (p^x - ip^y)/\sqrt{2}$ , and  $M_i m$  is the discretized  $p^+$  entering the diagram on leg  $i$ . These are the traditional Feynman diagram factors multiplied by  $a/8m\pi^{3/2}$

which comes from our rearrangement of propagator and vertex assignments. The  $1/p^+$  factors  $1/|M_3|$  or  $1/|M_1 M_2|$  are not included. We remind the reader that these are light-cone gauge ( $A_- = 0$ ) expressions and include the contributions that arise when the longitudinal field  $A_+$  is eliminated from the formalism.

The basic expressions for the complete quartic vertices, combining those from ‘‘Coulomb’’ exchange with those from the  $\text{Tr}[A_i, A_j]^2$  term in the Lagrangian, can be manipulated into a form that suggests a concatenation of two cubics. In Cartesian basis we can write them in the following way:

$$\begin{aligned} \Gamma^{i_1 i_2 i_3 i_4} &= \frac{g^2 a}{32m\pi^3} \left\{ \delta_{i_1 i_2} \delta_{i_3 i_4} \frac{(M_1 - M_2)(M_4 - M_3)}{(M_1 + M_2)^2} + (\delta_{i_1 i_3} \delta_{i_2 i_4} - \delta_{i_1 i_4} \delta_{i_2 i_3}) \right\} \\ &+ \frac{g^2 a}{32m\pi^3} \left\{ \delta_{i_2 i_3} \delta_{i_1 i_4} \frac{(M_1 - M_4)(M_2 - M_3)}{(M_1 + M_4)^2} + (\delta_{i_1 i_3} \delta_{i_2 i_4} - \delta_{i_1 i_2} \delta_{i_3 i_4}) \right\} \end{aligned} \quad (30)$$

Where as before all  $M_k$  are taken to flow *into* the vertex, and the rearrangement factor  $a/32m\pi^3$  has also been included. The first line on the r.h.s. looks like the exchange of an  $O(d)$  singlet and an  $O(d)$  antisymmetric tensor in the  $s$  channel (12,34) and the second line like the same exchanges in the  $t$  channel (23,41). It is easy to confirm in the case  $d = 2$  that these expressions are summarized in complex basis by the pair of diagrams

$$\begin{array}{c} \diagup \quad \diagdown \\ \diagdown \quad \diagup \end{array} = \frac{g^2 a}{32m\pi^3} \left( \frac{(M_1 - M_4)(M_2 - M_3)}{(M_1 + M_4)^2} + 1 \right) \quad (31)$$

$$\begin{array}{c} \diagdown \quad \diagup \\ \diagup \quad \diagdown \end{array} = \frac{g^2 a}{32m\pi^3} \left( \frac{(M_1 - M_4)(M_2 - M_3)}{(M_1 + M_4)^2} + \frac{(M_1 - M_2)(M_4 - M_3)}{(M_1 + M_2)^2} - 2 \right) \quad (32)$$

We next explain how the transverse momentum factors can be handled in our worldsheet construction. Recall that our scheme for spreading the propagator among  $M$  bits, involved the integral

$$I = \int d^2 q_1 \cdots d^2 q_{M-1} \exp \left\{ -\frac{a}{2m} \sum_{i=0}^{M-1} (\mathbf{q}_{i+1} - \mathbf{q}_i)^2 \right\}. \quad (33)$$

It is not hard to show that insertion in the integrand of the factor  $[\mathbf{q}_l - \mathbf{q}_{l-1}]$ , where  $l$  labels the  $l$ th bit leads to:

$$\int d^2 q_1 \cdots d^2 q_{M-1} [\mathbf{q}_l - \mathbf{q}_{l-1}] \exp \left\{ -\frac{a}{2m} \sum_{i=0}^{M-1} (\mathbf{q}_{i+1} - \mathbf{q}_i)^2 \right\} = \frac{\mathbf{q}_M - \mathbf{q}_0}{M} I. \quad (34)$$

This is an identity for any  $l = 1, 2, \dots, M$ . For later use we quote the generating functions

$$\begin{aligned} \left\langle \exp \left\{ \sum_{i=1}^{M-1} J_i q_i \right\} \right\rangle &= \exp \left\{ \frac{m}{2a} \sum_i \frac{i(M-i)}{M} J_i^2 + \frac{m}{a} \sum_{i<j} \frac{i(M-j)}{M} J_i J_j \right. \\ &\quad \left. + \frac{q_M}{M} \sum_i i J_i + \frac{q_0}{M} \sum_i (M-i) J_i \right\} \end{aligned} \quad (35)$$

$$\left\langle \exp \left\{ \sum_{i=0}^{M-1} K_i (q_{i+1} - q_i) \right\} \right\rangle = \exp \left\{ \frac{m}{2a} \sum_i K_i^2 - \frac{m}{2aM} \sum_{i,j} K_i K_j + \frac{q_M - q_0}{M} \sum_i K_i \right\} \quad (36)$$

From the second of these we see immediately that two vertex insertions on the same time slice and on the same strip produce a “quantum fluctuation” contribution:

$$\langle (q_{i+1} - q_i)(q_{j+1} - q_j) \rangle = \left( \frac{q_M - q_0}{M} \right)^2 + \frac{m}{a} \left[ \delta_{ij} - \frac{1}{M} \right]. \quad (37)$$

These fluctuation terms cause two coincident cubics to behave as a quartic contact vertex, and must be carefully analyzed in the context of translating the Yang-Mills quartic vertices into our worldsheet language. Because the  $\Delta \mathbf{q}$  insertions on the three different worldsheet strips joined at a vertex are applied on two different time slices, we have the three possible contributions shown in Fig. 2. The a) and b) contributions lead to the quartic vertices required by the Yang-Mills Feynman rules.

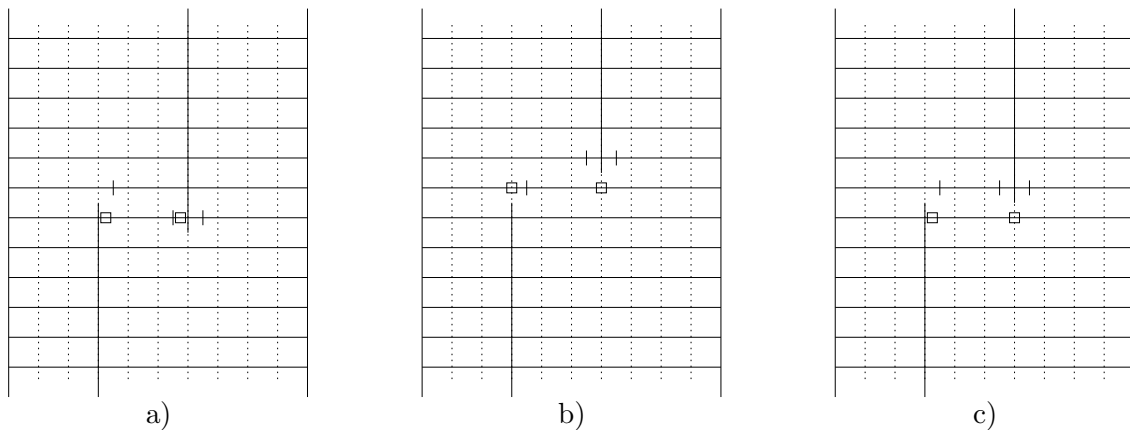


Figure 2: Possible contributions to the quantum term from two  $\Delta \mathbf{q}$  insertions placed at the location of the open squares on the same time slice. Figures a) and b) produce the desired quartic vertices. However c) is an artifact of our insertion procedure and must be suppressed. The tick marks identify the deleted ghost terms according to light-cone priority. The double deletion on strip 4 in figure c) provides a zero that suppresses this artifact.

To see how this works in a simple example, consider the four gluon diagrams built from two cubics in Fig. 3. The product of vertex factors is

$$\frac{g^2 a^2}{16m^2 \pi^3} M_2 M_4 \left( \frac{p_2^\vee + p_3^\vee}{M_2 + M_3} - \frac{p_3^\vee}{M_3} \right) \left( \frac{p_1^\wedge + p_4^\wedge}{M_1 + M_4} - \frac{p_1^\wedge}{M_1} \right). \quad (38)$$

In this process a fluctuation contribution of the type shown in Fig. 2a) comes from a double insertion on the intermediate string with momentum  $p_1 + p_4 = -p_2 - p_3$ . Remembering the  $1/|M_1 + M_4|$  factor from the intermediate propagator, the contribution of the quantum term is

$$\text{Quantum Term} = -2 \frac{g^2 a}{32m\pi^3} \frac{M_2 M_4 + M_1 M_3}{(M_1 + M_4)^2}, \quad (39)$$

where the  $M_1 M_3$  term comes from the diagram where the arrow on the intermediate line is reversed. Then one observes

$$-2(M_2 M_4 + M_1 M_3) = (M_1 - M_4)(M_2 - M_3) + (M_1 + M_4)^2. \quad (40)$$

The first term inserted in the numerator of Eq. 39 yields precisely the quartic vertex contribution from the induced instantaneous “Coulomb” exchange, and the second term yields precisely the

contribution of the commutator squared term in the Yang-Mills Lagrangian (see Eq. 31). It is not hard to confirm that the a) and b) type contributions correctly produce the quartic vertices for all other spin assignments to the external gluons.

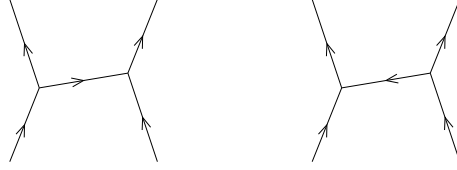


Figure 3: A four gluon amplitude

On the other hand contact interactions arising from contributions like Fig. 2c) are spurious and should not be included. We see that these spurious contributions arise when there is zero propagation time for the gluon exchanged between the two cubic vertices. The need to remove these spurious contributions is a strong argument to use our original ghost insertion scheme to account for  $1/p^+$  factors. Then the troublesome contact interaction is accompanied by the deletion of *two* ghost terms on the same time slice, which supplies a welcome zero. This doesn't happen for an alternative ghost insertion scheme based on spin flow mentioned later.

Now let's consider the worldsheet representation of the vertices of Eqs. 28, 29 in more detail. In the fusion case where 1 and 2 are incoming and 3 is outgoing. Let gluon 1 have  $M_1 = l$  and gluon 2 have  $M_2 = M - l$ . The vertex is represented by a strip of width  $M$ , the left boundary at  $i = 0$  and the right boundary at  $i = M$  and with a solid line coming in at  $i = l$ . Consider the time slice  $j = k$  just before the interaction point. Represent the insertion of a factor  $q_i^j$  by the notation  $\langle q_i^j \rangle$ . Then we have

$$\langle q_{l+1}^k - q_l^k \rangle = \frac{q_M - q_l}{M - l} = \frac{p_2}{M_2} \quad (41)$$

$$\langle q_l^k - q_{l-1}^k \rangle = \frac{q_l - q_0}{l} = \frac{p_1}{M_1} \quad (42)$$

Thus insertion of the factor  $q_{l+1} + q_{l-1} - 2q_l$  yields the desired vertex factor

$$\langle (q_{l+1}^k + q_{l-1}^k - 2q_l^k)^\wedge \rangle = \left( \frac{p_2^\wedge}{M_2} - \frac{p_1^\wedge}{M_1} \right). \quad (43)$$

When 3 and 1 are incoming, we have to put one insertion on the time slice  $k + 1$  and the other at the time slice  $k$ :

$$\langle q_{l+1}^k - q_l^k \rangle = \frac{q_M - q_l}{M - l} = \frac{p_1}{M_1} \quad (44)$$

$$\langle q_{l+1}^{k+1} - q_l^{k+1} \rangle = \frac{q_M - q_0}{M} = \frac{p_2}{M_2} \quad (45)$$

$$\langle q_{l+1}^{k+1} - q_l^{k+1} - q_{l+1}^k + q_l^k \rangle = \frac{p_2}{M_2} - \frac{p_1}{M_1}. \quad (46)$$

Similarly, when 2 and 3 are incoming

$$\langle q_l^k - q_{l-1}^k - q_l^{k+1} + q_{l-1}^{k+1} \rangle = \frac{p_2}{M_2} - \frac{p_1}{M_1}. \quad (47)$$

The fission cases where with one particle incoming and two outgoing are treated analogously.

### 3.2 Treatment of Remaining $p^+$ Factors

In order to suppress the spurious contact contributions of Fig. 2c), we choose the same ghost modifications at the vertex (to handle  $1/p^+$  factors) as in the scalar case (see Fig. 1). Then the factor of  $M_3$  of Eqs (28, 29) still needs to be represented locally on the world sheet. This seems to be very difficult unless we introduce yet more ghost degrees of freedom. One way to do this is to note that we are always free to introduce two “dummy” ghost systems,  $\beta, \gamma$  and  $\bar{\beta}, \bar{\gamma}$  whose net effect is to include a factor of unity in the path integral. On each time slice for each strip we choose the action as in Eq. 12 for  $\beta, \gamma$  and the one in Eq. 13 for  $\bar{\beta}, \bar{\gamma}$ . In other words on each time slice we insert

$$\int \prod_{i=1}^{M-1} d\gamma_i d\beta_i d\bar{\gamma}_i d\bar{\beta}_i \exp \left\{ \beta_1 \gamma_1 + \sum_{i=1}^{M-2} (\beta_{i+1} - \beta_i)(\gamma_{i+1} - \gamma_i) + \bar{\beta}_{M-1} \bar{\gamma}_{M-1} + \sum_{i=1}^{M-2} (\bar{\beta}_{i+1} - \bar{\beta}_i)(\bar{\gamma}_{i+1} - \bar{\gamma}_i) \right\} = 1. \quad (48)$$

Here we have dispensed with the factors of  $2\pi$  and  $a/m$  present in the  $b, c$  path integral. This insertion is completely harmless because it does nothing. But with these dummy-ghost systems available, we can locally produce factors of  $M_i$  at will as they are needed. For example, either  $e^{\beta_{M-1} \gamma_{M-1}}$  applied on the right of a strip of  $M$  bits or  $e^{\bar{\beta}_1 \bar{\gamma}_1}$  applied on the left of the strip produces a factor of  $M$ . At a vertex, the end of a solid line marks where two strips, 1 to the left of 2, join a single larger strip 3. Then an insertion of the first type on strip 1 produces  $M_1$ , of the second type on strip 2 produces  $M_2$ , and the sum of the two insertions produces  $M_1 + M_2 = -M_3$ . This scheme is perhaps over-generous in the number of dummy-ghosts introduced, but it serves to prove that a local description is possible.

As an aside, we briefly mention an alternative treatment of  $p^+$  factors assigned to vertices on the basis of spin rather than light-cone priority. In the complex basis  $(A_1 \pm iA_2)/\sqrt{2}$  each transverse propagator carries an arrow denoting the flow of spin. Suppose we associate the  $1/2|p^+|$  factor with the vertex at, say, the *tail*. Then there will always be enough denominator factors at each vertex to cancel all  $p^+$  factors in the numerator, leaving *at most* one  $p^+$  factor in the denominator. Again take  $p_k = M_k m$  to be the momentum flowing *in* to the vertex, so  $p_k^+ > 0 (< 0)$  if  $k$  is incoming (outgoing). The vertex in Eq. 28 will then receive the factor  $1/|M_3|$ , so it will be assigned the value

$$\begin{array}{c} \uparrow \\ \swarrow \quad \searrow \\ 1 \quad \quad 2 \end{array} \rightarrow \text{sgn}(p_3^+) \frac{ga}{4m\pi^{3/2}} \left( \frac{p_2^\wedge}{M_2} - \frac{p_1^\wedge}{M_1} \right) \quad (49)$$

and will have *no* leftover  $p^+$  factors. Contrast this with the vertex in Eq. 29, which receives the factor  $1/|M_1 M_2|$ :

$$\begin{array}{c} \downarrow \\ \swarrow \quad \searrow \\ 1 \quad \quad 2 \end{array} \rightarrow -\text{sgn}(p_1^+ p_2^+) \frac{ga}{4m\pi^{3/2}} \left( \frac{1}{M_1} + \frac{1}{M_2} \right) \left( \frac{p_2^\vee}{M_2} - \frac{p_1^\vee}{M_1} \right). \quad (50)$$

Here the  $p^+$  factors are always in the denominator and can thus be produced by modifying the  $b, c$  ghost action near the interaction point. The virtue of this alternative scheme is that all factors of  $p^+$

are accounted for without introducing extra ghosts. However, it leaves the problem of eliminating the spurious contact quartics arising from Fig. 2c) in some other way, because this alternate ghost arrangement provides no zero for that diagram. Diagram by diagram, one could discard it by hand, but to do it dynamically probably requires the introduction of extra ghost variables.

### 3.3 Polarization Flow Described by a Worldsheet Grassmann Field

To keep track of the flow of polarization indices for large diagrams we would like to introduce some worldsheet fermions, which in the absence of interactions do nothing more than reproduce the Kronecker delta, but in multi-loop diagrams reproduce the sum over all possible polarizations of internal lines.

We introduce worldsheet spinors of the Neveu-Schwarz-Ramond type,  $\mathbf{S}_k$ . Let us first evaluate some simple Grassmann integrals. Consider a single chain  $\mathbf{S}_1, \mathbf{S}_2, \dots, \mathbf{S}_{2K-1}, \mathbf{S}_{2K}$ , with an *even* number of spin variables, each carrying a transverse vector index and use the action

$$A = \sum_{i=1}^{2K-1} \mathbf{S}_i \cdot \mathbf{S}_{i+1}. \quad (51)$$

We shall define the measure for integration of the Grassmann variables by

$$\mathcal{D}S \equiv \prod_{i=1}^d [dS_{2K}^i dS_{2K-1}^i \cdots dS_1^i] \quad (52)$$

Then it is easy to check that

$$\int \mathcal{D}S e^A = 1 \quad (53)$$

$$\int \mathcal{D}S e^{A + \eta_1 \cdot \mathbf{S}_1 + \eta_{2K} \cdot \mathbf{S}_{2K}} = e^{\eta_{2K} \cdot \eta_1}. \quad (54)$$

In particular, the last equation implies

$$\int \mathcal{D}S S_1^k S_{2K}^l e^A = \delta_{kl}. \quad (55)$$

Note that these formulae *require* an even number of spins.

It is not hard to show that with an odd number of spins ( $2K + 1$  say)

$$\int \mathcal{D}S e^A = 0 \quad \text{for } 2K + 1 \text{ spins} \quad (56)$$

$$\int \mathcal{D}S e^{A + \eta_1 \cdot \mathbf{S}_1 + \eta_{2K+1} \cdot \mathbf{S}_{2K+1}} = \pm \prod_{i=1}^d (\eta_1^i + \eta_{2K+1}^i), \quad (57)$$

with the sign depending on the specific measure convention. In our worldsheet construction, we shall find that in order to guarantee the consistent application of the even spin formulae in the presence of interactions, the number of spins assigned to each bit must be a multiple of four.

For the propagator, we can assign one of the spin variables to each of the dots open or closed in Fig. 4. The open circles are where we will insert a factor  $S^i$  or  $S^j$ , so that the Grassmann integrals will yield the required Kronecker delta. It is interesting to write the formal continuum limit of the bulk part of the action to use in the propagator path integral. To do this we rename the four spins

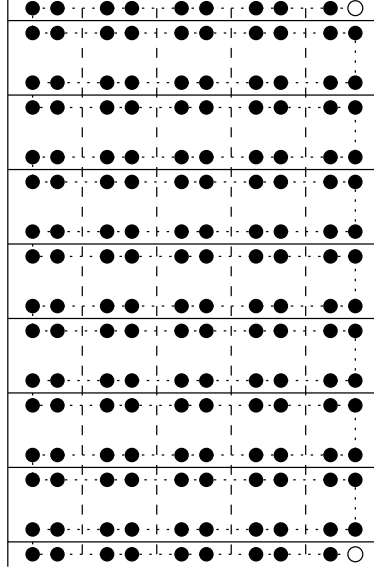


Figure 4: Assignment of Grassmann spins for propagator. Each dot is assigned a Grassmann spin  $\mathbf{S}$  and the bond pattern for the spin chain is indicated by dotted lines.

living on the  $i$ th bit on time slice  $j$  clockwise starting on the lower right hand corner:  $\mathbf{S}_{2i}^j$ ,  $\bar{\mathbf{S}}_{2i}^j$ ,  $\mathbf{S}_{1i}^j$ ,  $\bar{\mathbf{S}}_{1i}^j$ , respectively. Then, using the bond pattern implied by our spin chains, we find the bulk spin action

$$S_s = - \sum_{ij} \bar{\mathbf{S}}_{1i}^j \cdot (\mathbf{S}_{1i+1}^j - \mathbf{S}_{1i}^j) + \sum_{ij} \bar{\mathbf{S}}_{2i}^j \cdot (\mathbf{S}_{2i}^j - \mathbf{S}_{2i-1}^j). \quad (58)$$

In this form we easily read off the formal continuum limit. First identify continuum spin variables by the rule  $\mathbf{S}_{(1,2)i}^j \rightarrow \sqrt{a}\mathbf{S}_{1,2}(\sigma, \tau)$ , and similarly for  $\bar{\mathbf{S}}_{1,2}$ . Then we have the formal continuum limit

$$S_s \rightarrow \int d\tau d\sigma (\bar{\mathbf{S}}_2 \cdot \mathbf{S}'_2 - \bar{\mathbf{S}}_1 \cdot \mathbf{S}'_1). \quad (59)$$

where the prime denotes  $d/d\sigma$ . Note that although the bulk has a simple continuum limit, the accurate dynamical treatment at the boundaries heavily relies on the  $x^+, p^+$  lattice.

Next we turn to interactions. We draw the diagrams for the fusion and fission three gluon vertices in Fig. 5. First consider the fusion vertex. Label the external legs 1, 2, 3, ordered counter-clockwise starting at the lower left. The three open circles mark the spins that participate in the vertex insertion that should yield the correct Yang-Mills cubic vertex. Note that the insertion will be cubic in spin variables and hence Grassmann odd. This is necessary because we have inserted a single spin variable on each external line to represent the polarization of the external gluon. In the fusion case, starting at the lowest point and working counter-clockwise around the triangle, call these spins  $\mathbf{S}_A$ ,  $\mathbf{S}_B$ , and  $\mathbf{S}_C$  respectively. Finally, let  $k$  label the time slice just before the solid line ends and let  $l$  label the spatial location of the solid line. Then, with ghost modifications according to light-cone priority, the vertex insertion will be

$$\frac{\bar{\mathcal{V}}}{2\pi} = (\mathbf{u} \cdot \mathbf{S}_A \mathbf{S}_B \cdot \mathbf{S}_C + \mathbf{v} \cdot \mathbf{S}_B \mathbf{S}_C \cdot \mathbf{S}_A + \mathbf{w} \cdot \mathbf{S}_C \mathbf{S}_A \cdot \mathbf{S}_B) \exp \left\{ -\frac{a}{m} (b_{l+1}^{k+1} - b_l^{k+1})(c_{l+1}^{k+1} - c_l^{k+1}) \right\}. \quad (60)$$

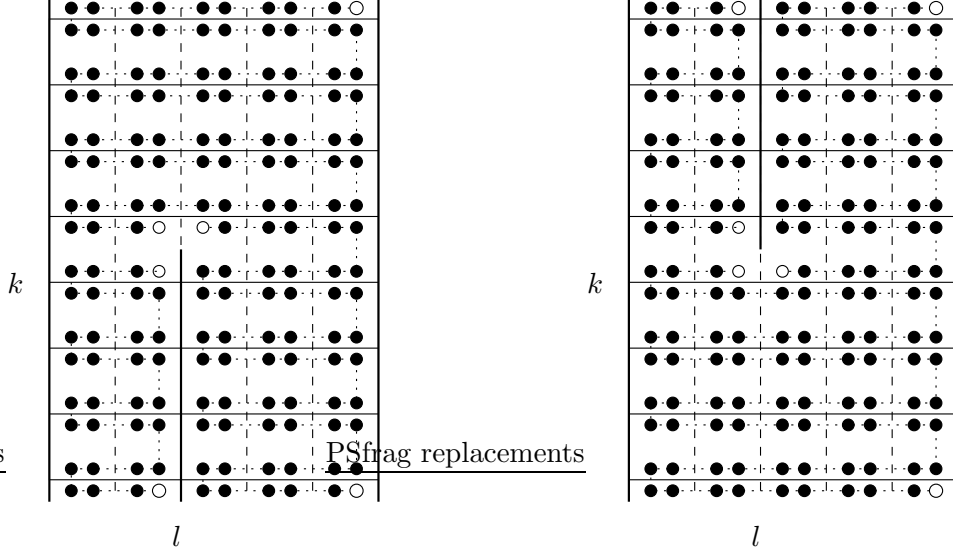


Figure 5: Cubic fusion and fission vertices.

Here  $\mathbf{u}$ ,  $\mathbf{v}$ , and  $\mathbf{w}$  can be determined from Eqs. 28, 29 by writing out the coefficient on the r.h.s. in complex basis<sup>‡</sup>:

$$\begin{aligned}
& \mathbf{u} \cdot \mathbf{S}_A \mathbf{S}_B \cdot \mathbf{S}_C + \mathbf{v} \cdot \mathbf{S}_B \mathbf{S}_C \cdot \mathbf{S}_A + \mathbf{w} \cdot \mathbf{S}_C \mathbf{S}_A \cdot \mathbf{S}_B \\
&= (u+v)^\wedge S^\vee_A S^\vee_B S^\wedge_C + (u+v)^\vee S^\wedge_A S^\wedge_B S^\vee_C + (v+w)^\wedge S^\wedge_A S^\vee_B S^\vee_C \\
&+ (v+w)^\vee S^\vee_A S^\wedge_B S^\wedge_C + (u+w)^\wedge S^\vee_A S^\wedge_B S^\vee_C + (u+w)^\vee S^\vee_A S^\wedge_B S^\vee_C
\end{aligned} \tag{61}$$

from which we infer

$$\mathbf{u} + \mathbf{v} = \frac{ga}{4m\pi^{3/2}} p_3^+ \left( \frac{\mathbf{p}_2}{p_2^+} - \frac{\mathbf{p}_1}{p_1^+} \right) \tag{62}$$

$$\mathbf{v} + \mathbf{w} = \frac{ga}{4m\pi^{3/2}} p_1^+ \left( \frac{\mathbf{p}_3}{p_3^+} - \frac{\mathbf{p}_2}{p_2^+} \right) \tag{63}$$

$$\mathbf{w} + \mathbf{u} = \frac{ga}{4m\pi^{3/2}} p_2^+ \left( \frac{\mathbf{p}_1}{p_1^+} - \frac{\mathbf{p}_3}{p_3^+} \right). \tag{64}$$

As already stated, the  $\mathbf{p}_i/p_i^+$  can be produced by insertions of  $\Delta\mathbf{q}$  at strategic locations near the interaction point:

$$\frac{\mathbf{p}_1}{M_1} \rightarrow \mathbf{q}_l^k - \mathbf{q}_{l-1}^k, \quad \frac{\mathbf{p}_2}{M_2} \rightarrow \mathbf{q}_{l+1}^k - \mathbf{q}_l^k, \quad \frac{\mathbf{p}_3}{M_3} \rightarrow \mathbf{q}_l^{k+1} - \mathbf{q}_{l-1}^{k+1}. \tag{65}$$

The remaining factors of  $p_i^+$  can then be supplied by dummy ghost insertions

$$M_1 \rightarrow e^{\beta_{l-1}^k \gamma_{l-1}^k}, \quad M_2 \rightarrow e^{\bar{\beta}_{l+1}^k \bar{\gamma}_{l+1}^k}, \quad M_3 \rightarrow -e^{\beta_{l-1}^k \gamma_{l-1}^k} - e^{\bar{\beta}_{l+1}^k \bar{\gamma}_{l+1}^k} \tag{66}$$

For the fission case, starting from the bottom left open circle of the triangle and working around the triangle counter-clockwise, call the inserted spins  $\mathbf{S}_D$ ,  $\mathbf{S}_E$ , and  $\mathbf{S}_F$  respectively. Also

<sup>‡</sup>Incidentally, referring to Eq. 61, the rule using the spin to dictate the assignment of the  $1/p^+$  factors from the propagators can be simply stated:  $S_k^\wedge \rightarrow S_k^\wedge/|M_k|$  but  $S_k^\vee \rightarrow S_k^\vee$ .

the *incoming* momenta are assigned counter-clockwise, starting with the bottom leg,  $p_1$ ,  $p_2$ ,  $p_3$  respectively. Then the vertex insertion will have the similar structure

$$\frac{\mathcal{V}}{2\pi} = (\mathbf{u} \cdot \mathbf{S}_D \mathbf{S}_E \cdot \mathbf{S}_F + \mathbf{v} \cdot \mathbf{S}_E \mathbf{S}_F \cdot \mathbf{S}_D + \mathbf{w} \cdot \mathbf{S}_F \mathbf{S}_D \cdot \mathbf{S}_E) \exp \left\{ -\frac{a}{m} (b_{i+1}^{k+1} c_{i+1}^{k+1} + b_{i-1}^{k+1} c_{i-1}^{k+1}) \right\} \quad (67)$$

with the same expressions for  $\mathbf{u}$ ,  $\mathbf{v}$ , and  $\mathbf{w}$ , but a different representation of the  $p_i^+$  factors

$$M_3 \rightarrow -e^{\beta_{i-1}^{k+1} \gamma_{i-1}^{k+1}}, \quad M_2 \rightarrow -e^{\bar{\beta}_{i+1}^{k+1} \bar{\gamma}_{i+1}^{k+1}}, \quad M_1 \rightarrow e^{\beta_{i-1}^{k+1} \gamma_{i-1}^{k+1}} + e^{\bar{\beta}_{i+1}^{k+1} \bar{\gamma}_{i+1}^{k+1}} \quad (68)$$

For the purposes of writing a formula for the sum of all planar diagrams, as in Eq. 23, it is better to use a Grassmann even version of the vertex insertion. A simple way to do this is to add a component  $S^{d+1}$  to the spin variables  $\mathbf{S}$ , making the spin a vector in  $d+1$  dimensions. Then  $S^{d+1}$  can be used to represent the Kronecker delta with even variables (see Eq. 55):

$$\int DS S_1^k S_1^{d+1} S_{2K}^{d+1} S_{2K}^l = \delta_{kl}. \quad (69)$$

When one uses the even insertions  $S^k S^{d+1}$  on incoming external lines and  $S^{d+1} S^k$  on outgoing external lines, then everything goes through as before provided we use the Grassmann even vertex insertions.

$$\mathcal{V}_e \equiv \mathcal{V} S_D^{d+1} S_E^{d+1} S_F^{d+1}, \quad \bar{\mathcal{V}}_e \equiv S_A^{d+1} S_B^{d+1} S_C^{d+1} \bar{\mathcal{V}}. \quad (70)$$

Note that we have normalized  $\mathcal{V}_e$  and  $\bar{\mathcal{V}}_e$  so that they will appear in the expression for the sum of all planar diagrams with exactly the same coefficients as with the scalar case.

## 4 Concluding Remarks

In this article we have shown how to extend the worldsheet construction of Ref. [1] to the case of Yang-Mills theories. This extension requires the introduction of a worldsheet fermionic spin variable  $\mathbf{S}$  to account for the flow of gluon spin through complicated diagrams.

Although we have not explicitly written out the rather unwieldy analog for Yang-Mills of Eq. 23, the formula summing planar diagrams, we have completely specified all of its ingredients. To construct the corresponding formula for Yang-Mills, one first includes in  $S$  the action of the spin variables (58) and the dummy ghost variables (see 48). Next, one must add terms in the exponent corresponding to the second and third lines of (23) that rearrange the bond patterns of the new spin and ghost variables appropriately in the neighborhood of each solid line. Finally, for  $\mathcal{V}_0$  and  $\bar{\mathcal{V}}_0$  one substitutes the Yang-Mills Grassmann even versions of these quantities  $\mathcal{V}_e$  and  $\bar{\mathcal{V}}_e$  given in (70).

As we have already discussed, the quartic vertices of the Yang-Mills light-cone gauge Feynman diagrams are automatically produced by the fluctuation contribution of two  $\Delta \mathbf{q}$  insertions when they occur on the same time slice and on the same strip. Thus the formula for the sum of all planar diagrams for Yang-Mills closely follows the scalar  $\text{Tr} \phi^3$  paradigm. We draw a couple of four gluon diagrams in Fig. 6, and it should be evident how they are represented in the worldsheet formalism.

However, this is not the end of the story because we know that the continuum limit involves divergences that require renormalization. It will be very interesting to see how the renormalization program can be carried out using our world sheet language. The  $x^+, p^+$  lattice we have used in our construction is identical to that in Ref. [5, 6] where one loop diagrams are studied in some detail.

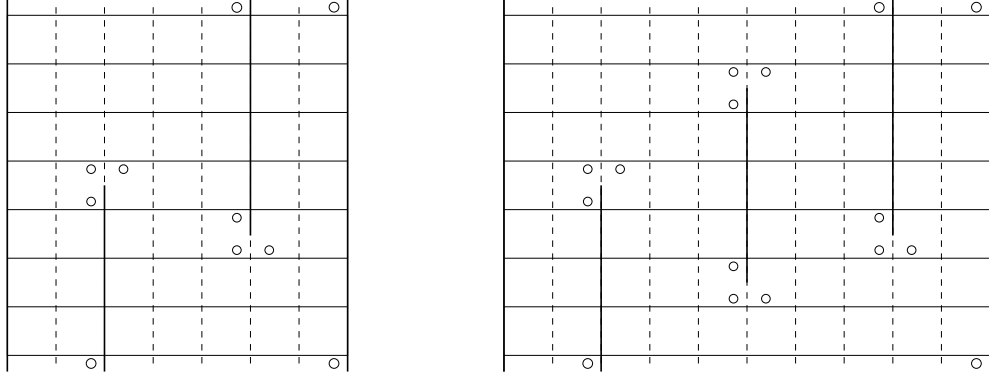


Figure 6: Four gluon diagram comprised of two cubics and a one loop diagram. Only the spin insertion locations are shown; those in the bulk have been suppressed.

The worldsheet version of these calculations will only differ in the treatment of end points of the sums over discretized  $x^+, p^+$  locations of the vertices. For example, the self-energy counter-term required to ensure that the gluon stay massless in perturbation theory has been explicitly worked out in [5]. It is clear that such counter-terms will have the structure of “short loops”, *i.e.* vertical solid lines on the world sheet spanning a small number of lattice sites. However, we leave the analysis of renormalization and determination of the necessary counter-terms in the worldsheet formalism for future work.

Another direction for future research is to repeat the construction for supersymmetric field theories. In particular, it will be very interesting to do this for  $\mathcal{N} = 4$  supersymmetric Yang-Mills theory in the limit  $N_c \rightarrow \infty$ . This is the theory Maldacena has conjectured is dual to type IIB string theory on  $AdS_5 \times S_5$  [7–9]. The worldsheet sigma model corresponding to this proposal can be analyzed in the strong ’t Hooft coupling limit  $N_c g_s^2 \rightarrow \infty$ , but it becomes a strong coupling theory in the opposite limit  $N_c g_s^2 \rightarrow 0$ . Our construction, which would have parallels to one previously proposed by Nastase and Siegel [10], would give a two dimensional worldsheet system that is tied to this opposite limit. Maldacena duality should then mean that our worldsheet system is dual to the  $AdS_5 \times S_5$  sigma model worldsheet system. Such a duality would be fascinating to discover.

Acknowledgments: I would like to thank K. Bardakci for the many valuable insights he shared in our first collaboration, and for his valuable comments on this work. I thank J. Sonnenschein for useful discussions and for reading the manuscript. Finally I acknowledge useful discussions with D. Berenstein, I. Klebanov, J. Maldacena, A. Polyakov and M. Strassler. This work was supported in part by the Monell Foundation and in part by the Department of Energy under Grant No. DE-FG02-97ER-41029.

## References

- [1] K. Bardakci and C. B. Thorn, *Nucl. Phys.* **B626** (2002) 287, hep-th/0110301.
- [2] G. ’t Hooft, *Nucl. Phys.* **B72** (1974) 461.
- [3] S. Mandelstam, *Nucl. Phys.* **B64** (1973) 205; *Phys. Lett.* **46B** (1973) 447; *Nucl. Phys.* **B69** (1974) 77; see also his lectures in *Unified String Theories*, ed. M. Green and D. Gross (World Scientific) 1986.

- [4] R. Giles and C. B. Thorn, *Phys. Rev.* **D16** (1977) 366.
- [5] K. Bering, J. S. Rozowsky and C. B. Thorn, *Phys. Rev.* **D61** (2000) 045007, hep-th/9909141.
- [6] S. Gudmundsson and C. B. Thorn, “One Loop Calculations in Gauge Theories Regulated on as  $x^+ - p^+$  Lattice”, in preparation.
- [7] J. M. Maldacena, *Adv. Theor. Math. Phys.* **2** (1998) 231-252, hep-th/9711200.
- [8] E. Witten, *Adv. Theor. Math. Phys.* **2** (1998) 253-291 hep-th/9802150.
- [9] S. S. Gubser, I. R. Klebanov, and A. M. Polyakov, *Phys. Lett.* **B428** (1998) 105, hep-th/9802109.
- [10] H. Nastase and W. Siegel, *JHEP*, 0010:040 (2000), hep-th/0010106.